Presented at the 32nd European PV Solar Energy Conference and Exhibition, 20-24 Juni 2016, München, Germany

CZ SILICON BENCHMARK FOR P-TYPE PERC SOLAR CELLS

Pierre Saint-Cast, Isolde Reis, Johannes Greulich, Sabrina Werner, Elmar Lohmüller, Hannes Höffler, Jonas Haunschild and Ralf Preu
Fraunhofer Institute for Solar Energy Systems ISE, Heidenhofstraße 2, 79110 Freiburg, Germany
Telephone: +49 761 4588 5480, fax: +49 761 4588 9000, e-mail: pierre.saint-cast@ise.fraunhofer.de

ABSTRACT: In this paper, seven Czochralski and one Float Zone *p*-type silicon materials, were processed as PERC solar cells in the Fraunhofer ISE PVTEC pilot line. In order to compare materials with different bulk resistivity, the rear contact distance was varied in order to keep the spreading resistance in the same range. As-processed and regenerated, energy conversion efficiencies from 20.5% until 21.0% were achieved for each material. Within processing- and measurement accuracy, all materials performed on the same level when comparing the solar cells performance. Implied open circuit voltage samples revealed to be more sensitive to the material quality than the solar cells and give some more details. Due to the small differences in the results, we will not provide a ranking of the material tested in this paper. However all the materials tested here are capable of at least 20.7%, when applied in a PERC solar cell process. A larger number of materials would be necessary in order for this study to be representative of the Cz wafer market.

Keywords: PERC, Cz material, light induced degradation

1 INTRODUCTION

During recent years, impressive progress was made in increasing the solar cell conversion efficiency as well as in decreasing the cost of crystalline silicon solar cell fabrication. This was made possible thanks to great efforts along the whole value chain of crystalline silicon solar cells, including silicon feedstock, solar cell processing and module fabrication. Today, industry is rapidly moving towards the "Passivated Emitter and Rear Cell" (PERC) structure which allows conversion efficiencies well above 20% and has been in the focus of research and development for more than 15 years [1,2,3]. An increased spreading of high efficiency solar cells brings up and emphasizes the need for high quality silicon material.

This paper presents a quality comparison of commercially available p-type monocrystalline Cz-grown silicon material. Fraunhofer ISE organized a benchmark to determine the best Cz-Si material for p-type PERC solar cells. The results show that the material tested in this study is capable of yielding high efficiencies with the potential for further process optimization.

2 MATERIAL PRETEST

2.1 Eligibility and wafer specification

In order to take part in this benchmark the participants had to provide monocrystalline silicon wafers for the photovoltaic industry based on Czochralski growth method, the participants who are manufacturing wafers for microelectronics application and retailers were not accepted.

The wafers accepted for this test had to meet the specification listed in Table I. A pretest was carried out in order to verify whether the wafers meet the specification or not.

2.2 Participation and pretest

Cz material manufacturers all over the world were invited to participate to this benchmark. Seven suppliers answered the call and were capable of supplying wafers according to the specification. Reference material used as standard material in our pilot was also added to the test. The reference material used was *p*-type magnetic-Czochralski grown with a bulk resistivity value of about $\rho_{bulk} \approx 1.4\ \Omega$ cm.

The suppliers were numbered in order to anonymize the participant of the benchmark. The material numbers 1 to 7 correspond to the suppliers which took part in the benchmark, the material number 8 corresponds to the reference material. The numbers are consistent throughout the paper.

Before processing the wafers to solar cells, a pretest was applied to all of the provided wafers in order to verify if the wafers meet the specified criteria and to find correlations to solar cell results. The following values were measured inline: thickness (on 3 tracks), resistivity (one track), saw marks, effective lifetime (MDP-method [4]). In addition, the following methods were also applied: photoluminescence imaging (PL), infrared imaging for the detection of micro-cracks, and optical inspection in order to detect: stains, edge defects and geometry.

Table I: Wafer specific requirement in order to participate to the test.

Item / Measurement	**Specification**	**Unit**
Material	Silicon	-
Method	Czochralski growth	-
Doping Type	*p*-type Si Boron or Gallium doped	-
Orientation	<100>	
Resistivity	0.5-3.0	Ω cm
Resistivity variation	± 0.5	Ω cm
Oxygen Content	as low as possible	atoms/cm^3
Carbon Content	< 5.0 x 10^{16}	atoms/cm^3
Iron Content	< 2.0 x 10^{10}	atoms/cm^3
Lifetime	as high as possible (> 20)	µs
Size	156.0 ± 0.5	mm
Diameter	Pseudo square : 200.0 ± 0.5 Full square : 219.0 ± 0.5	mm
Etch Pit Density (EPD)	≤ 3000	cm^{-2}
Average Wafer Thickness	180 ± 20	µm
Total Thickness Variation (TTV)	≤ 30	µm
Saw Mark Depth	≤ 15	µm
Cracks/Holes	no	-
Edge Defects/Chips	no defects > 0.5	mm
Surface Condition	as cut, cleaned, no stains	-

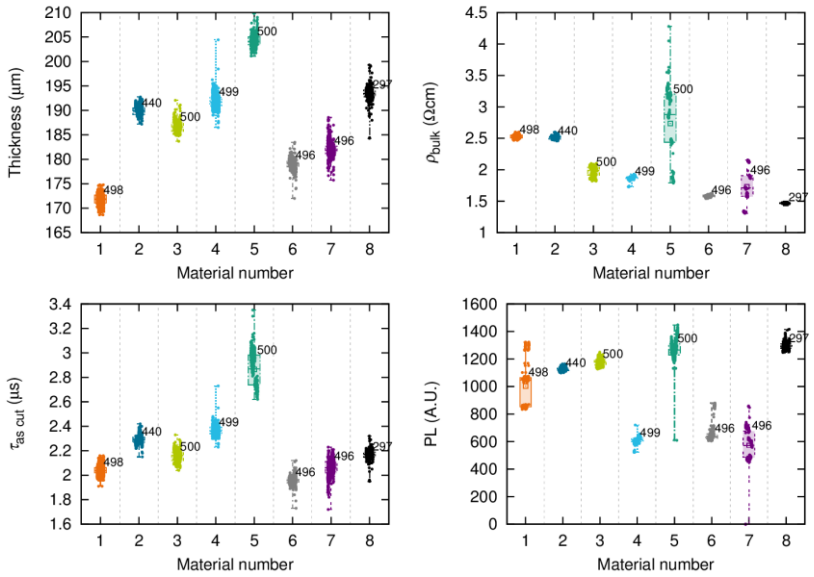

Figure 1 Selected results of the pretest applied to the wafers of all suppliers (material number 1-7) and the reference material (number 8). All results were within the expected variations.

A part of the results of the pretest is displayed in Figure 1. The thickness, the resistivity (ρ_{bulk}), the effective carrier lifetime of the as cut wafers ($\tau_{as\ cut}$), and the intensity of the PL signal during PL imaging. The results from the resistivity are needed later in order to adapt the distance (or pitch) between the rear line contacts. The value of $\tau_{as\ cut}$ and of PL are limited due to surface recombination. Despite that, these values might be correlated with the electrical quality of the material and are given as an indication.

At this stage, several suppliers did not meet exactly all of our criteria:

- Material number 2 is Float Zone (FZ) material and not Czochralski grown.
- Material number 5 has a resistivity from 2 Ω cm to 3.5 Ω cm, however the accepted variation of the resistivity was maximal 0.5 Ω cm (see Table I). Selected wafers were used for further processing.
- Material number 7 is pseudo square and has a diameter of 205 mm. Our specification for pseudo square material was a diameter of 200 mm. No screen printing mask for the front and the rear side was available for this format. Therefore, these wafers were processed further as if they were 200 mm diameter.

Due to the resonable number of participants, no supplier was excluded from the benchmark and all materials were fully processed and characterized.

2 SOLAR CELL PROCESSING AND CHARACTERISATION

2.1 Processing

The solar cells were completely processed in the industry-related PV-TEC pilot line at Fraunhofer ISE [5]. Commercially available industrial tools are used for each of the solar cell fabrication processes. The process flow is presented in Figure 2.

Figure 2 Process flow used for the fabrication of the PERC solar cells.

The wafers are first labeled with laser-marking for tracing and randomized in groups of 10 wafers in order to minimize the influence of process fluctuations on the out coming results. After an alkaline saw-damage removal, the wafers are alkaline-textured and the rear side is chemically polished resulting in a thickness reduction of about 40 µm in total. The homogeneous emitter is formed in a tube furnace diffusion process using $POCl_3$. Directly following the diffusion, an oxidation is performed in-situ [6]. Then, a wet-chemical edge isolation (CEI) is carried out in order to remove the emitter on the rear side. Prior passivation, a wet cleaning (SC1/SC2 [7]) is carried out. The passivation of the rear surface is obtained by a 6 nm-thick aluminum oxide (Al_2O_3) layer which is deposited by fast atomic layer deposition (ALD). The ALD deposition is followed by an annealing step performed in a tube furnace under N_2 atmosphere at 550°C for 10 min. A silicon oxide (SiO_x, 100 nm thick) and silicon nitride (SiN_y, 100 nm thick) layer stack serve as capping layers. The capping layers are deposited by plasma enhanced chemical vapor deposition (PECVD). Concerning the front surface passivation, a PECVD SiN_z layer is used. All the processes applied up to this stage will be later referred to as the "front-end".

Then, the formation of the metal contacts is carried out. The rear layers are opened using a laser process in

order to obtain a line-shaped local contact opening (LCO). The front and rear side metallization is processed by screen printing. The front grid features five busbars and a finger distance of 1.56 mm with a printed finger width wf ≈ 55-70 µm. The rear electrode does not feature Ag/Al soldering pads. Finally, the contact firing is performed in an industrial conveyor belt furnace and the solar cells are measured with an industrial cell tester.

In addition to the solar cells, special test samples were made. Implied open circuit voltage (iV_{OC}) samples correspond to wafers, with only the front-end processes being applied. These samples are then directly fired without laser opening or screen printing processes. These samples allow determining the V_{OC} potential independent of the metal recombination losses. Emitter saturation current (j_{0e}) samples mirror symmetrically on both front and back side the front surface of the iV_{OC} samples. The j_{0e} samples are also fired without metal. iV_{OC} samples and j_{0e} samples were measured using quasi-steady-state photoconductance (QSSPC [8]) method.

2.1 Pitch variation

Materials with different base resistivity need to be processed with different contact distances on the rear (pitch) in order to yield the same efficiency. Our approach to meet the processing condition is a variation of the pitch. First, the materials were separated in three different categories:

- Low resistivity, from 1.25 Ω cm until 1.75 Ω cm. The materials 6, 7 and 8 belong to this category.
- Middle resistivity, from 1.75 Ω cm until 2.25 Ω cm. The materials 3 and 4 belong to this category.
- High resistivity, from 2.25 Ω cm until 3 Ω cm. The materials 1, 2 and 5 belong to this category.

Each category has its own pitch variation. Each pitch has been chosen in order to keep the spreading resistance within a range of 0.15 Ω cm^2 to 0.25 Ω cm^2. In Fig. 3, the spreading resistance is given as a function of wafer resistivity and the pitch, for an effective contact width of 55 µm and a wafer thickness of 150 µm. The spreading resistances presented in Fig 3 were calculated using an analytical model [9]. In table II the pitch variation for each category is given.

In addition to the pitch variation, a firing temperature variation was performed, so that from the initial 63 wafer per material processed only 7-8 wafers were processed identically (the size each group might vary due to breakage).

4 RESULTS AND DISCUSSION

4.1 Other measurements

The measurement of the emitter saturation current (j_{0e}) shows a very good repeatability between the materials. The medians value of j_{0e} varies between 79 fA/cm^2 and 85 fA/cm^2 and the standard deviation is about 8 fA/cm^2 for all materials. It can be expected that the emitter behaves similarly for the different materials. In addition, to the j_{0e} values these samples also deliver information on the bulk lifetime by fitting the invert effective carrier lifetime. The median lifetime extracted varies between 300 µs and 1000 µs. Although this lifetime difference appears to be significant, it can be explained by the large bulk doping variation between the materials. Thus it cannot be directly correlated with the V_{OC} potential of the solar cells within this experiment.

Table II: Distance between the rear contacts lines (pitch) used for each resistivity category.

Resistivity category	low	middle	high
Resistivity range [Ω cm]	1.25-1.75	1.75-2.25	> 2.25
Pitch 1 [µm]	1000	800	600
Pitch 2 [µm]	1200	1000	800
Pitch 3 [µm]	1400	1200	1000

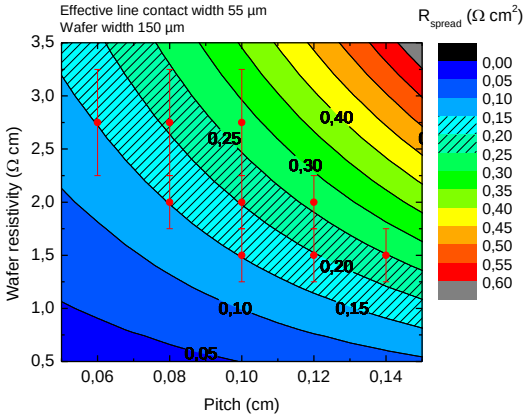

Figure 3 Spreading resistance (R_{sperad}) as a function of the wafer resistivity and the distance between the rear contacts (pitch). The calculations were done supposing a wafer thickness of 150 µm and an effective contact width of 55 µm.

The maximal implied V_{OC} is a more appropriate value. This value corresponds to the maximal implied V_{OC} allowed by the front half of the solar cell which includes the recombination at the emitter and half of the recombination in the bulk. This value corresponds to the iV_{OC} at an irradiance equivalent to 2 suns of the j_{0e} samples. The results are presented in Fig. 4.

The implied open circuit voltage (iV_{OC}) was measured on the iV_{OC} samples (see section 2.2). The iV_{OC} value measured corresponds to the potential of the front-end without the recombination due to the metallization. More specifically the iV_{OC} sample includes the recombination at the emitter in the bulk and on the passivated rear surface. The iV_{OC} results are presented in Fig. 5. These results correlate very well with the ones presented in Fig. 4. As mentioned earlier, the j_{0e} values are very similar between the materials. Therefore, the difference in iV_{OC} between the groups can be mainly

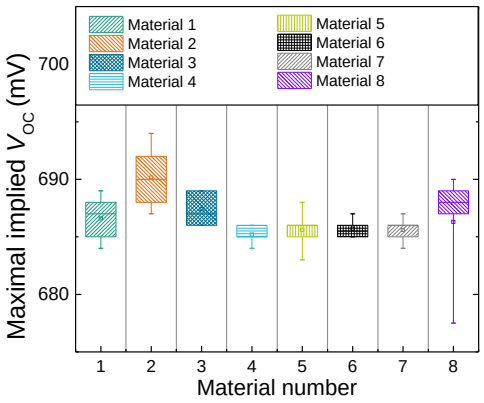

Figure 4 Implied V_{OC} at an irradiance equivalent to 2 suns of j_{0e} samples, which corresponds to the maximal implied V_{OC} allowed by the front the solar cell and half of the bulk.

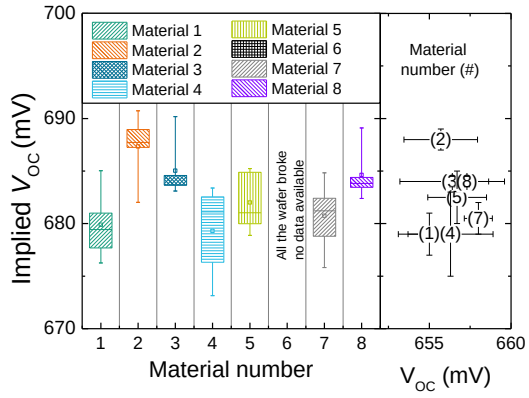

Figure 5 On the left hand side, the implied V_{OC} at irradiation equivalent to 1 suns of iV_{OC} samples, which corresponds to the V_{OC} allowed by the front-end process of the solar cell. On the right hand side, the implied V_{OC} as a function of the measured V_{OC} of the solar cells from the same material.

attributed to the material quality. A variation up to 10 mV was observed for the iV_{OC} samples, the variations in V_{OC} are much smaller (see Fig. 6). These variations do not to correlate with the V_{OC} variation of the solar cells. Therefore it seems that for this experiment, the performance before metallization does not correlate with the performances after metallization. This could be explained by instabilities in the metallization process influencing the recombination parameters.

4.2 Influence of the pitch

From the three firing temperatures applied, two led to a noticeable decrease in the solar cell performance, indicating that the process window was relatively small. Thus, only the results of the solar cells fired at the lowest temperature will be presented. In Fig. 6 the results of the illuminated current voltage measurement are given. The measurement was performed directly after processing (as-processed). The energy conversion efficiency (η), the fill factor (FF), the short circuit current (j_{SC}) and the open circuit voltage (V_{OC}) are given for the material 1-8 and for each pitch.

The efficiencies obtained are ranging from 20.5% to 21.0%. For each material, the variation of the pitch has a noticeable impact on the efficiency of more than 0.2%. The expected impact of the pitch is the following:

- For a large pitch, the series resistance increases and therefore the FF decreases. However, the rear recombination decreases and therefore the V_{OC} increases. A small increase of the j_{sc} can also be expected due to the increase of the internal reflection.
- For a small pitch, the effect is opposite, the FF increases, the V_{OC} decreases and the j_{sc} decreases slightly.
- The overall impact cannot be estimated as they have opposite impacts on the efficiency and we do not know the details of each individual effect.

The expected behavior can be observed for most of the materials. For materials 1, 2 and 3 the V_{OC} clearly increases with the pitch, for the materials 4, 5 and 6 the largest pitch has the highest V_{OC} values, however the trend is unclear for the lower pitch. For the materials 7 and 8 no clear correlation to V_{OC} can be found. For the materials 1-5 and 7 the FF clearly decreases with the pitch as expected. For the materials 6 and 8 no clear difference can be observed between the pitch 2 and 3. Concerning the j_{sc} no clear trend can be observed in the results and its variation might be related to process instabilities. In general the pitch related behavior of V_{OC} and FF are not consistent with the expectation in all cases and are probably also related to process fluctuations. As all materials seem to have a different optimal pitch, the results of each material will be treated independently from the pitch.

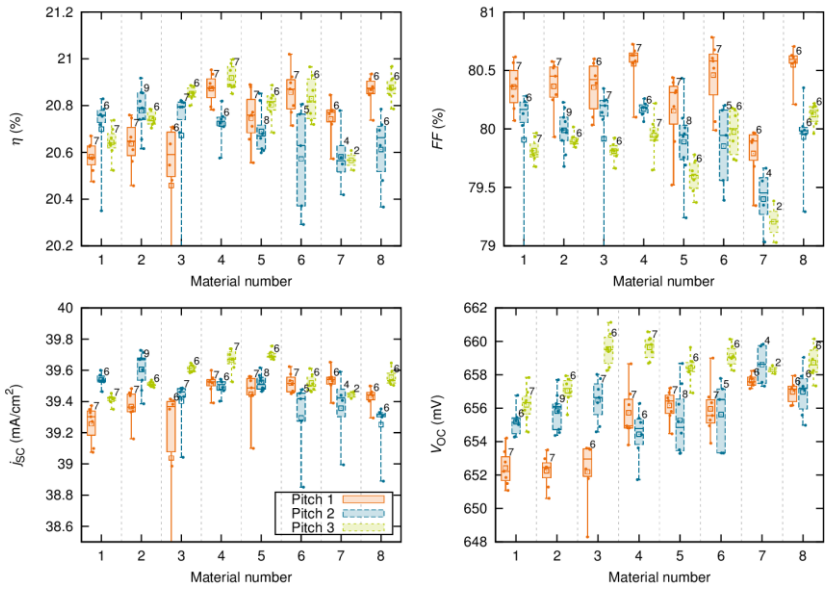

Figure 6 Results of the illuminated current voltage measurement for the lowest firing temperature applied. The material 1 to 8 and all the pitches are displayed. The measurement was performed directly after processing. Between the end of the process and the measurement, the cells were kept in a dark environment.

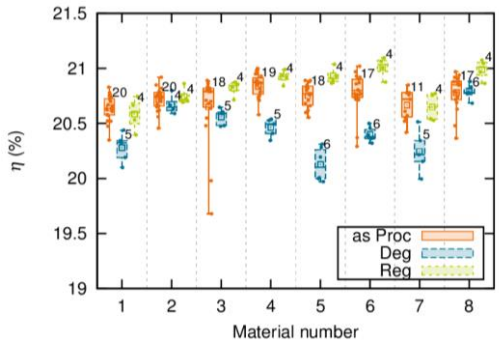

Figure 7 Energy convention efficiencies as the function of the material for the as process (as Proc), the degraded (Deg) and regenerated (Reg) state.

4.3 Light induced degradation and regeneration

Light induced degradation (LID) is very important to consider when studying the quality and performance of *p*-type Cz material. Five wafers representative of each material (close the median efficiency of the material) were selected in order to study the effect of LID on the material. After processing (as Proc), the selected solar cells were degraded (Deg) during 96 h under controlled irradiation. Then, the solar cells were regenerated (Reg) at 140°C under 1 sun irradiation during 2 hours. For each group a test sample was regenerated for an additional hour in order to check the completeness of the regeneration. No substantial improvement was observed, therefore after 2 hours the regeneration can be considered being completed. After regeneration the solar cells were degraded again for 96 h to verify the stability of the regenerated results and no significant change in efficiency could be measured. The efficiency in the as-processed, degraded and regenerated state are presented in Fig. 7.

As it could have been expected, the materials 2 and 8 did not show any significant degradation, which is explained by the low oxygen concentration of Float Zone and magnetic Cz material. The other materials degraded from 0.5%$_{abs}$ until 0.9%$_{abs}$ efficiency. This value did not correlate with the doping concentration, which tends to show that the oxygen concentration also varies among the material. It is difficult to predict which state is the most representative of the field condition. Recent studies tend to show that a complete degradation is too pessimistic and that a kind of regeneration process takes place naturally in the field. In addition, fast stabilization processes are now under development for industrial production, which could greatly reduce the impact of LID [11]. In a future benchmark, the use of fast regeneration would allow to obtain better statistical results after regeneration.

Although there are noticeable differences for the materials after regeneration, these results are based on only 4 samples per group. Due to the lack of statistical significance, we will abstain here from giving a ranking of the suppliers. A larger experiment should be conducted to verify the results including a regeneration of all the samples. It seems that the level of sensitivity required to resolve clearly the impact of material quality was not reached for the PERC solar cells in this experiment. However the efficiencies obtain are representative of actual efficiencies reach in production [12]. In fact, all the materials received in this experiment allowed for similar efficiencies (as-Pros or Reg) compare to the high quality magnetic Cz (Material 8), which tend to show that all the materials have also a high quality. In order to increase the sensitivity on solar cell level, a more stable PERC solar cell process with higher efficiency potential should be applied [13].

It is interesting to notice that difference in efficiencies between the materials is 0.4%$_{abs}$ in the regenerated stat and 1.0%$_{abs}$ in the degraded stat, therefore fast regeneration could be used in a production line, in order to level the difference in the incoming material quality.

5 CONCLUSION

Wafers from seven different *p*-type monocrystalline silicon material suppliers, in majority Cz, were processed as PERC solar cells. Except from the pitch, all materials were used without adapting the process. Energy conversion efficiencies from 20.5% until 21.0% were achieved in the as-processed state and confirmed via regeneration. This result shows the stability and flexibility of the PERC process used in this experiment.

The material performance observed on solar cell level was on a very similar level within measurement accuracy. However, more sensitive iV_{OC} and j_{0e} differences between the materials. Two deductions follow, first the quality of all the materials used in this experiment allowed for after-regeneration efficiencies close to the high quality magnetic Cz reference, second the cell process applied here was not sensitive enough to resolve clearly the differences in the material performance for such high material quality.

We will therefore abstain from giving a ranking of the suppliers because the quantity tested and the differences detected were too small to be representative of the Cz wafer market. However, it can be stated that all the materials tested here are capable of at least 20.7%, when applied in a PERC solar cells process.

ACKNOWLEDGEMENTS

The authors would like to thank all colleagues at the Fraunhofer ISE Photovoltaic Technology Evaluation Center (PV-TEC), the companies which send material and make this benchmark possible: Ubiquity Solar, Norwegian Crystals and others companies. This work was funded by the German Federal Ministry for Economic Affairs and Energy within the project "CUT-A" under contract no. 0325823.

REFERENCES

[1] A. W. Blakers, A. Wang, A. M. Milne, J. Zhao and M. A. Green, "22.8% efficient silicon solar cell", Applied Physics Letters, 55(13), 1363–1365 (1989).
[2] Press realise PV magazine Trina 16th Dec. 2015, Solar World 14th Jan. 2016, Gintech 5th Jan. 2016
[3] T. Dullweber, H. Hannebauer, U. Baumann, T. Falcon, K. Bothel, S. Steckemetz, R. Brendel, "Fine-Line Printed 5 Busbar PERC Solar Cells With Conversion Efficiencies Beyond 21%" 30th EU PVSEC, Paris, France, Sep. 2014.
[4] K. Dornich *et al.*, "New spatially resolved inline lifetime metrology on multicrystalline silicon for pv" 24th EUPVSEC, Hamburg, Germany, pp. 1106–1108.

[5] D. Biro, R. Preu, S. W. Glunz, S. Rein, J. Rentsch, G. Emanuel et al., "PV-Tec: Photovoltaic technology evaluation center - design and implementation of a production research unit", Proceedings 21st EUPVSEC 2006, pp. 621–624.
[6] S. Werner et al. Procedings 29th EU PVSEC, 2014, pp. 1342.
[7] Kern, W. et al., RCA Review, Vol. 31, pp. 187-205, 1970.
[8] R. A. Sinton and A. Cuevas, Appl. Phys. Lett, vol. 69, no. 17, pp. 2510–2512, 1996.
[9] P. Saint-Cast, Ph.D. Thesis, Physic, Constance University, pp. 61, 2012.
[10] P. Saint-Cast *et al.*, "Analysis of the losses of industrial-type PERC solar cells". to be published.
[11] A. Herguth *et al.*, "Accelerating Boron-Oxygen Related Regeneration: Lessons Learned from the BORNEO Project" 30th EUPVSEC, Hamburg, Germany, 2015, pp. 804-807
[12] B. Tjahjono et al., Proceedings 28th EUPVSEC, Paris, France (2013), pp. 775
[13] H. Neuhaus, PVCellTech Conference, Kuala Lumpur, Malaysia (2016)